The Astrophysical Journal, 778:180 (5pp), 2013 December 1 doi:10.1088/0004-637X/778/2/180

CROSS-FIELD DIFFUSION OF ENERGETIC (100 keV to 2 MeV) PROTONS IN INTERPLANETARY SPACE

Edio da Costa Jr.[1], Bruce T. Tsurutani[2], Maria Virgínia Alves[3], Ezequiel Echer[3], and Gurbax S. Lakhina[4]
[1] Instituto Federal de Minas Gerais-IFMG, Ouro Preto, MG, 35400-000, Brazil; edio.junior@ifmg.edu.br, costajr.e@gmail.com
[2] Jet Propulsion Laboratory, California Institute of Technology, Pasadena, CA 91109, USA
[3] Instituto Nacional de Pesquisas Espaciais-INPE, São José dos Campos, SP, 12227-010, Brazil
[4] Indian Institute for Geomagnetism, Navi Mumbai 410 218, India
Received 2013 July 27; accepted 2013 October 12; published 2013 November 13

ABSTRACT

Magnetic field magnitude decreases (MDs) are observed in several regions of the interplanetary medium. In this paper, we characterize MDs observed by the *Ulysses* spacecraft instrumentation over the solar south pole by using magnetic field data to obtain the empirical size, magnetic field MD, and frequency of occurrence distribution functions. The interaction of energetic (100 keV to 2 MeV) protons with these MDs is investigated. Charged particle and MD interactions can be described by a geometrical model allowing the calculation of the guiding center shift after each interaction. Using the distribution functions for the MD characteristics, Monte Carlo simulations are used to obtain the cross-field diffusion coefficients as a function of particle kinetic energy. It is found that the protons under consideration cross-field diffuse at a rate of up to ≈11% of the Bohm rate. The same method used in this paper can be applied to other space regions where MDs are observed, once their local features are well known.

Key words: diffusion – magnetic fields – methods: data analysis – methods: numerical – Sun: heliosphere

Online-only material: color figure

1. INTRODUCTION

The interaction of energetic charged particles with magnetized plasmas remains one of the most fundamental problems in space and astrophysical plasma physics. This particle–field interaction plays an essential role in solar energetic particle transport in the heliosphere (Shalchi et al. 2006), shock acceleration of particles both in interplanetary (Li et al. 2003; Zank et al. 2000, 2006) and astrophysical shocks, and cosmic-ray modulation and propagation in the interstellar medium (Shalchi et al. 2006). In most plasmas, the ambient magnetic field, $\boldsymbol{B}_0$, sets a preferred direction for energetic charged particle propagation, and an additional random or turbulent magnetic field component induces transport. Unperturbed orbits, computed in terms of B_0 alone, are the starting point for quasilinear theory, which has dominated the conceptualization of particle transport for more than 30 yr. If one assumes a diffusive motion of the particles, then the parallel and perpendicular diffusion coefficients can be calculated to describe the motion within the plasma (see, e.g., Shalchi 2009). The diffusion coefficients have been derived following different theoretical approaches, e.g., quasilinear approximations (Jokipii 1966), a hard-sphere scattering model (Gleeson 1969), and nonlinear guiding center theories (Matthaeus et al. 2003; Shalchi 2009), among others. Dosch et al. (2009) have discussed the relationship between different theories for the cosmic-ray diffusion. In particular, cross-field particle transport is believed to arise from diffusive or fractionally diffusive processes (del Castillo-Negrete 2006), and thus inherently involves a decorrelation process either associated with collisions or wave-particle interactions.

Recently, Shalchi (2010) presented a new nonlinear theory for cosmic-ray scattering across the mean magnetic field. He concluded that this new theory can explain subdiffusive transport for slab turbulence and recover the nonlinear standard theory for field line wandering as a special limit. Shalchi (2009) investigated charged particle scattering in the limit of strong turbulence. In that paper, it is shown that the Bohm limit is the correct limit for strong turbulence.

In this paper, we deal with the cross-field diffusion of energetic charged particles resulting from their interaction with magnetic dips called magnetic decreases, or MDs. The main effect of a charged particle interaction with an MD is the cross-field diffusion due to particle guiding center displacements (Tsurutani et al. 1999; Tsurutani & Lakhina 2004; Costa Jr. et al. 2011). We emphasize that an interaction between a particle and an MD is a nonresonant process, and differs substantially from wave–particle interactions. We compare the numerical diffusion coefficient that we obtain with a Bohm-like diffusion coefficient appropriated for a highly variable magnetic field magnitude (strong turbulence) given by $D_B = (\omega_{ci}/16)r_L^2$ (Hasegawa & Tsurutani 2011), where r_L is the unperturbed Larmour radius.

MDs are depletions in the magnitude of the interplanetary magnetic field (IMF) of up to 90% of the ambient magnetic field (B_0) and are convected by the solar wind. They are pressure balance structures filled with hot plasma where the magnetic pressure decreases are supplanted by plasma thermal pressure increases (Winterhalter et al. 1994; Tsurutani et al. 2002a). MD sizes range from a few to thousands of proton gyroradii or more, assuming the gyroradius of a ≈1 keV proton (Tsurutani et al. 2009). They are observed at different heliocentric distances and at both low and high heliospheric latitudes (Turner et al. 1977; Burlaga & Lemaire 1978; Winterhalter et al. 1994; Tsurutani et al. 1999, 2009, 2010; Franz et al. 2000).

We focus on MDs detected by the *Ulysses* spacecraft instrumentation over the solar south pole. In the solar polar regions, the solar wind is usually characterized by pure coronal hole fast streams (Tsurutani et al. 2011), and MDs are convected by the wind at speeds of ≈750–800 km s^{-1}. For those regions where there are no stream–stream interactions (Neugebauer 1999), one proposed mechanism of MD formation is the evolution of large amplitude right-hand polarized Alfvén wave packets propagating at large angles to the IMF (Buti et al. 2001). Tsurutani et al. (2002a, 2002b, 2005) have suggested that thermal proton acceleration due to Alfvén wave damping creates MDs by a diamagnetic effect.

A geometrical model to describe energetic particle/MD interactions was presented by Tsurutani et al. (1999) and Tsurutani & Lakhina (2004). More recently, Costa Jr. et al. (2011) used Monte Carlo simulations to obtain the displacement of the particle guiding centers perpendicular to the magnetic field. Here, we present the perpendicular diffusion coefficient ($D_\perp$) as a function of the proton energy associated with a large number of MDs observed by *Ulysses* in 1994, in its first pass over the south pole of the Sun. We first empirically characterize these MDs and then perform Monte Carlo simulations of the interaction of energetic protons with these structures to obtain $D_\perp$. These Monte Carlo simulations, first suggested by Tsurutani et al. (1999), confirm the rough estimate of a cross-field diffusion coefficient of $\approx 0.1\ D_B$ presented by Tsurutani et al. (2005).

2. DATA

MD events used in this study were observed by *Ulysses* when it first passed over the south pole of the heliosphere ($\approx -80^\circ$ and ≈ 2.3 AU from the Sun) in 1994. Figure 1 shows 27 days (days 242–268 of 1994) of magnetic field data from *Ulysses*. Panel (A) of Figure 1 shows one-minute averaged IMF magnitudes, presenting a typical result of MD studies: many magnetic field decreases of various amplitudes but very few magnetic field increases (Tsurutani et al. 1999). Panels (B)–(D) of Figure 1 show the three components of the IMF with the same time resolution. The coordinate system is *RTN*, where $\hat{R}$ points radially outward from the Sun and $\hat{T} = \hat{\Omega} \times \hat{R}/|\hat{\Omega} \times \hat{R}|$, where $\hat{\Omega}$ is the rotation axis of the Sun. The third vector, $\hat{N}$, completes the right-hand system. Finally, panel (E) shows four to eight minutes of averaged solar wind speed. At that time, the region was dominated by a high speed ($\approx$750–800 km s^{-1}) solar wind emanating from a polar coronal hole (Phillips et al. 1994).

For the interval of data presented in Figure 1, 129 MDs were identified with magnetic field amplitude decreases greater than 20% of B_0. These events were plotted as a histogram and were curve-fitted to obtain the empirical size, magnetic field MD, and occurrence frequency distribution functions (Tsurutani et al. 1999). The parameters used for fitting are the MD diameter in km, dm, and the relative field decrease $dB = 1 - B_{\rm MD}/B_0$, where $B_{\rm MD}$ is the minimum magnetic field magnitude within the MD. The values have been fitted by exponentials and the percentage of events, Y_{dm} and Y_{dB}, are given below (Tsurutani et al. 1999; Costa Jr. et al. 2011):

$$Y_{dm} = 38.5e^{-1.5\times10^{-5}dm}, \quad (1)$$

and

$$Y_{dB} = 5.4 + 348.7e^{-8dB}. \quad (2)$$

Burlaga & Lemaire (1978) noticed that some of the MDs had little or no magnetic field directional changes across them. They called these linear events. Figure 2 shows an example of a linear MD with high-resolution 1 s averaged data. The event was detected during day 246 of 1994. The three components of the IMF and the magnetic field magnitude are shown. As can be seen by the figure, there are minor magnetic field directional changes across the MD. However, the magnetic field magnitude returns to approximately the same value after the event.

3. MODEL AND RESULTS

We use a geometrical model to calculate the guiding center displacement after a charged particle and an MD nonresonantly interact (Tsurutani et al. 1999; Tsurutani & Lakhina 2004). Figure 3(A) gives a schematic of this interaction. The particle gyroradius is r, the impact distance is d (the distance between the center of the particle gyromotion and the center of the MD), and the magnetic field is directed into the plane.

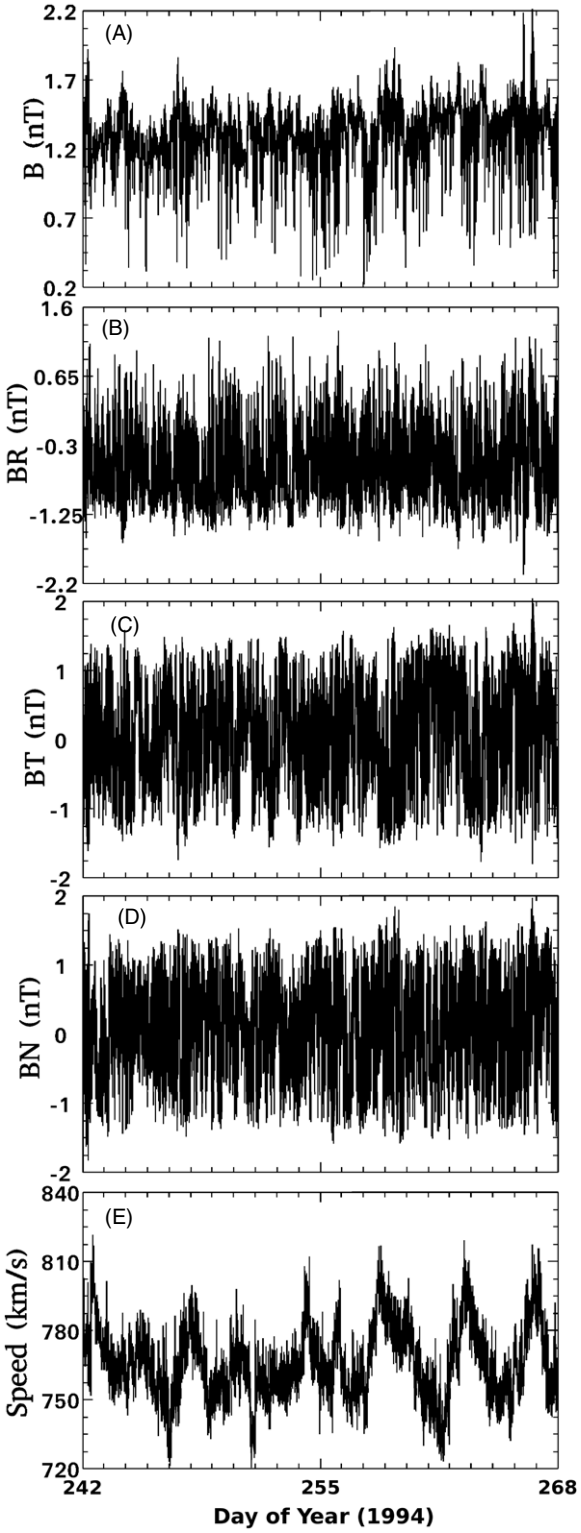

Figure 1. Twenty seven days of one-minute averaged IMF magnitudes obtained by *Ulysses* over the south pole of the Sun in 1994, in nT: panels (A) magnetic field magnitude, (B) B_R component, (C) B_T component, and (D) B_N component. Panel (E) 27 days of four to eight minutes averaged solar wind speed (km s^{-1}).

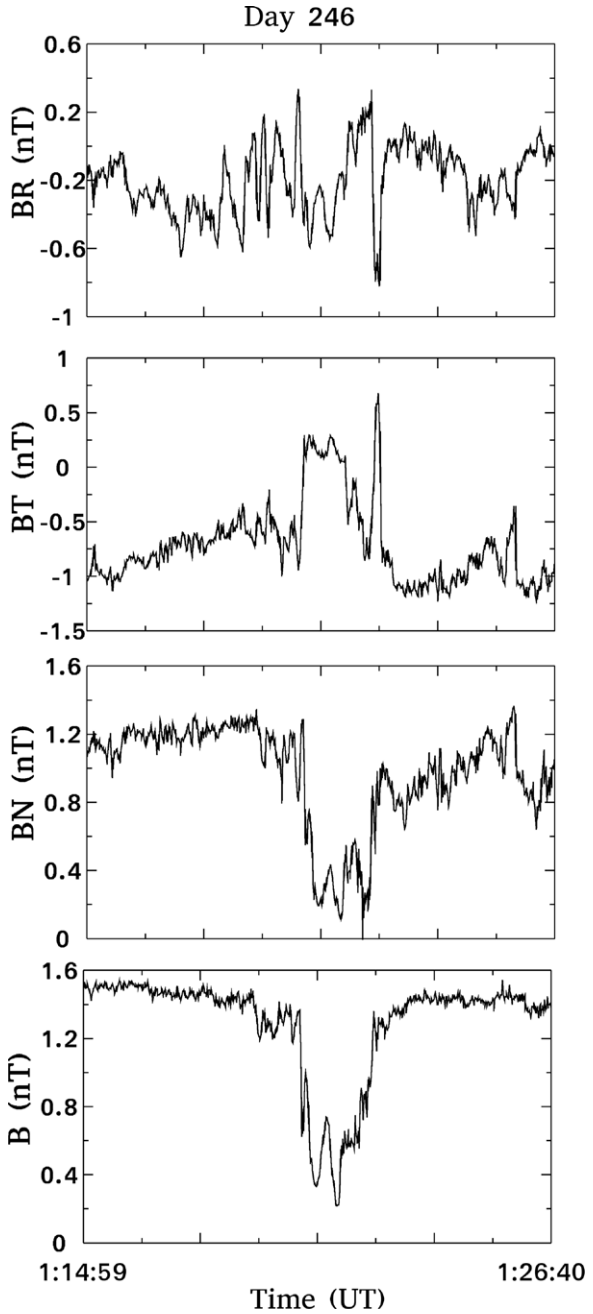

Figure 2. Example of a linear MD where there are small magnetic field directional changes within the structure.

For simplicity, we assume that the MDs have a circular cross-section of radius a, given by $dm/2$, and a cylindrical geometry in a three-dimensional view aligned along the magnetic field. The magnetic field magnitude inside the MD is assumed to be constant with no change in angle, so the model will apply to linear MDs. The other parameters, such as the decrease of the magnetic field inside the MD and the size of the MD, are obtained from *Ulysses* observations. The MD radii detected for the time interval studied and used in this paper range from $\approx 1.2 \times 10^3$ to $\approx 2 \times 10^5$ km, while the Larmour radii of the energetic particles with energies of 100 keV to 2 MeV range from $\approx 3.2 \times 10^4$ to $\approx 1.5 \times 10^5$ km, respectively, considering a 45° pitch angle. These values are for the unperturbed Larmour radii, while the particles move in the assumed unperturbed field, outside the MDs.

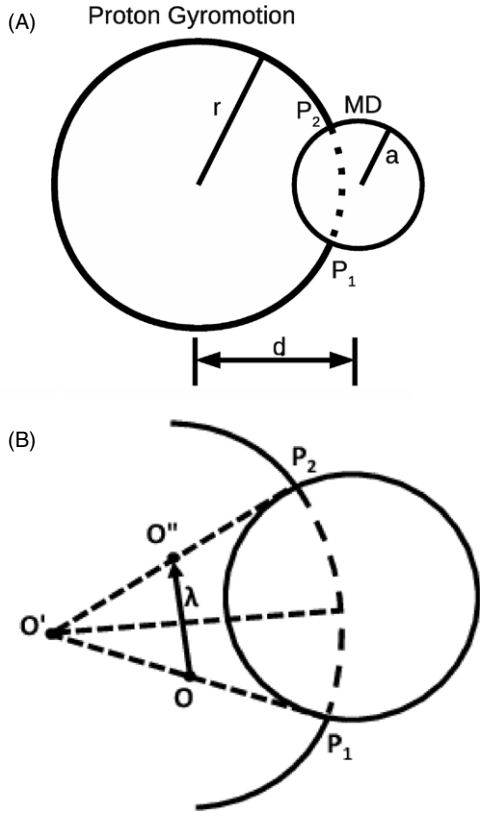

Figure 3. ((A) and (B)) Geometry of the interaction of a charged particle of gyroradius r and an MD of radius a. The other symbols are explained in the text. Adapted from Tsurutani et al. (1999).

Figure 3(B) shows how the guiding center of a charged particle is displaced perpendicular to the magnetic field due to the interaction with the MD. The particle initially moves in the ambient field $\boldsymbol{B}_0$ from the bottom upward, and its gyrocenter is located at point O. The interaction with the MD takes place at point P_1. Due to the decrease in the ambient magnetic field within the MD, from B_0 to $B_{\rm MD}$, the particle gyrocenter becomes the point O'. Inside the MD, the gyroradius is given by $r' = r(B_0/B_{\rm MD})$. After leaving the MD at point P_2, the new gyrocenter is located at point O''. The net result of the interaction is that the guiding center of the particle has moved from point O to point O''. The latter is shown in Figure 3(B) by the symbol λ. The diffusion distance λ is given by the expression (Costa Jr. et al. 2011):

$$\lambda = \frac{2(m-1)}{m} \times \left[a^2 - \frac{(a^2 + d^2 + r^2(1-2m) + (m-1)(-a^2 + d^2 + r^2))^2}{4(d^2 + r^2(m-1)^2 + (m-1)(-a^2 + d^2 + r^2))} \right]^{\frac{1}{2}}, \quad (3)$$

where $m = B_0/B_{\rm MD}$.

Equation (3) was obtained assuming that there are no significant changes of the field direction within the regions inside and outside of the MD. Our assumption is based on numerous observations in space plasmas showing that under special circumstances, the magnetic field MDs are not accompanied by changes in the field vector directions (Winterhalter et al. 1994; Tsurutani et al. 2009, 2011).

We use Equation (3) and Monte Carlo simulations to obtain the cross-field diffusion coefficients as a function of particle

kinetic energy resulting from energetic proton nonresonant interactions. In the Monte Carlo model, we select three parameters randomly: (1) the impact parameter, (2) the scale size of the MD, and (3) the depth of the decrease in the magnetic field magnitude. Two other parameters are handled by making separate runs: (4) the particle energy and (5) the particle pitch angle.

We first select a proton kinetic energy E. The ambient field magnitude was assumed to be $B_0 = 1.2$ nT, defining the proton unperturbed gyroradius r, assuming a pitch angle of 45°. The proton interactions with "N" different MDs are simulated by solving Equation (3) "N" times. For each interaction, it is necessary to assign values of a, m, d, and the proton–MD phase angle (θ). The values for a ($=dm/2$) and m ($= B_0/B_{\rm MD}$) are taken from Equations (1) and (2), respectively, using the Metropolis–Hastings rule with symmetric selection rates (Amar 2006; Costa Jr. et al. 2011). The Monte Carlo method (MCM) was used to sample as accurately as possible the properties of the MDs from statistical distributions. The MCM consists of starting with a random initial value for a variable (we call it initial state i). After this, a possible new value is selected for the variable (the possible new state j). The new state can be accepted with probability $P_{ij}^{\rm acc}$ or can be rejected with probability $1-P_{ij}^{\rm acc}$. The Metropolis–Hastings rule with symmetric selection rates for the selection of the values is given by $P_{ij}^{\rm acc} = \min(1, P_j/P_i)$, where P_j is the value of the distribution function as calculated for state j and P_i is the value calculated for state i. The process is repeated until the necessary number of values is selected.

Finally, the impact parameter d is randomly selected in the range where the interaction is possible ($|r-a| < d < |r+a|$) and the proton–MD phase angle is randomly selected between 0 and 2π, which means that the interactions can occur at any point on the particle's trajectory.

In the simulation runs, each proton interacts with 100 MDs, solving Equation (3) for each interaction. The simulations were run 1000 times with the MDs selected by the Monte Carlo Metropolis–Hastings approach. For each of the 1000 runs, a value of the net guiding center displacement (λ_i) was determined. The 1000 values of λ_i were later used to calculate the cross-field diffusion coefficient. A second set of runs was performed using 200 MDs with the purpose of studying the stability of the simulation approach. It was concluded that 100 MD interactions gave stable results. The Monte Carlo simulations were repeated for proton energies varying from 100 keV to 2 MeV, with energy steps of 100 keV. All of the particles simulated are considered to be non-relativistic.

Finally, the perpendicular diffusion coefficient for the nonresonant interactions is obtained by

$$D_\perp = \frac{\langle \Lambda^2 \rangle}{2\Delta t}, \tag{4}$$

where $\langle \Lambda^2 \rangle = \sum_{i=1}^{1000} \lambda_i^2/1000$ and Δt is the average time between interactions. The parameter Δt depends on the distance between adjacent MDs and on the proton parallel speed. The distances between MDs were obtained empirically using the solar wind convection speed $V_{\rm SW}$. Thus, Δt is given by

$$\Delta t = \frac{V_{\rm SW} t_s}{N_{\rm MD}} \left(\frac{1}{V_\parallel} \right), \tag{5}$$

where t_s is the total data interval time in seconds, $N_{\rm MD}$ is the number of MDs detected within this interval, and $V_\parallel$ is the particle speed parallel to $\boldsymbol{B}_0$, again assuming a pitch angle of 45°. The numerator of the diffusion coefficient ($\langle \Lambda^2 \rangle$) depends on the proton perpendicular energy and the denominator ($2\Delta t$) depends on the proton parallel energy. The parallel velocity component is important for timing the interactions between successive MDs. As the MDs are of finite sizes, the time interval between interactions with adjacent MDs is much larger than the time duration of a particle–MD interaction.

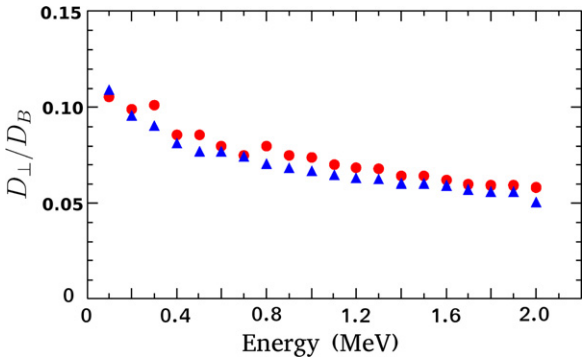

Figure 4. Ratio between the obtained perpendicular diffusion coefficient ($D_\perp$) and Bohm diffusion coefficient (D_B). The circles represent 100 particle–MD interactions and the triangles represent 200 interactions.

(A color version of this figure is available in the online journal.)

Results for the perpendicular diffusion coefficient ($D_\perp$) normalized by the Bohm diffusion coefficient (D_B) are shown in Figure 4 as a function of proton energies. The circular points in Figure 4 correspond to the 100 interaction simulations and the triangles to the 200 interaction simulations. The value of $D_\perp/D_B$ is ≈0.11 for $E \approx 100$ keV and monotonically decreases to ≈0.055 at $E \approx 2$ MeV. The slope of the curve approaches zero at $E = 2$ MeV. From the results in Figure 4 it can be expected that cross-field diffusion will continue for $E > 2$ MeV at the same rate.

4. DISCUSSION AND CONCLUSION

Cross-field diffusion resulting from interactions between energetic protons and linear MDs was investigated using a geometrical model and a Monte Carlo approach. It was found that for 45° pitch angles, the cross-field diffusion of 100 keV protons will occur at a rate of ≈11% of D_B and of 2 MeV protons at a rate of ≈5.5% of D_B.

Similar diffusion processes may occur in other space and astrophysical situations where there are large magnetic field magnitude changes. Here, we have used MDs as an example. It is possible that diffusion at compressive waves near heliospheric shocks or astrophysical shocks (Duffy 1992; Jokipii 1992; Dosch et al. 2011) may occur if either the waves or MDs are found to exist near these structures. In the case of MDs, it is thought that nonlinear wave processes (Tsurutani et al. 2002a; Buti et al. 2001) create the magnetic decreases. The interaction of energetic protons that we consider here is a parasitic process.

The method presented in this paper can be employed to calculate the cross-field diffusion of heavy ions and electrons and for other space regions where MDs are present, such as interplanetary space at low latitudes, planetary magnetosheaths, interplanetary shocks, heliospheric sheaths, and astrophysical plasmas. However, it is necessary to take into account the features of the MDs in the regions of interest.

Tsurutani et al. (2009) have recently shown that compressive mirror mode (MM) structures occur in the sheath region of heliospheric shocks. Although MMs and MDs are different

mechanisms (Tsurutani et al. 2010), similar to linear MDs, MMs are characterized by decreases in the magnitude of the magnetic field, without significant angular rotation. Our model have not been tested yet with these compressive magnetic structures. However, we could expect that the cross-field diffusion through MMs will occur at the same rate we obtained here for MDs.

The Brazilian authors thank the Brazilian agencies Conselho Nacional de Desenvolvimento Científico e Tecnológico (CNPq-projects 140441/2006-9, CNPq/PQ 301233/2011-0, and 305373/2012-2), Coordenação de Aperfeiçoamento de Pessoal de Nível Superior (CAPES), and Fundação de Amparo à Pesquisa do Estado de São Paulo (FAPESP-project 2008/01288-0) for financial support. Portions of this research were carried out at the Jet Propulsion Laboratory, California Institute of Technology under contract with NASA. G.S.L. thanks the National Academy of Sciences, India, for support under NASI-Senior Scientist Platinum Jubilee Fellowship and FAPESP (2012/05397-3) for a Visiting Professor fellowship.

REFERENCES

Amar, J. G. 2006, CSE, 8, 9
Burlaga, L. F., & Lemaire, J. F. 1978, JGR, 83, 5157
Buti, B., Tsurutani, B. T., Neugebauer, M., & Goldstein, B. E. 2001, GeoRL, 28, 1355
Costa, Jr. E., Echer, E., Alves, M. V., et al. 2011, JASTP, 73, 1405
del Castillo-Negrete, D. 2006, PhPl, 13, 082308
Dosch, A., Shalchi, A., & Tautz, R. C. 2011, MNRAS, 413, 2950
Dosch, A., Shalchi, A., & Weinhorst, B. 2009, AdSpR, 44, 1326
Duffy, P. 1992, A&A, 262, 281
Franz, M., Borgess, D., & Horbury, T. S. 2000, JGR, 105, 12725
Gleeson, L. J. 1969, P&SS, 17, 31
Hasegawa, A., & Tsurutani, B. T. 2011, PhRvL, 107, 245005
Jokipii, J. R. 1966, ApJ, 146, 480
Jokipii, J. R. 1992, ApJL, 393, L41
Li, G., Zank, G. P., & Rice, W. K. M. 2003, AdSpR, 32, 2597
Matthaeus, W. H., Qin, G., Bieber, J. W., & Zank, G. P. 2003, ApJL, 590, L53
Neugebauer, M. 1999, RvGeo, 37, 107
Phillips, J. L., Balogh, A., Bame, S. J., et al. 1994, GeoRL, 21, 1105
Shalchi, A. 2009, APh, 31, 237
Shalchi, A. 2010, ApJL, 720, L127
Shalchi, A., Bieber, J. W., Matthaeus, W. H., & Schlickeiser, R. 2006, ApJ, 642, 230
Tsurutani, B. T., Dasgupta, B., Galvan, C., et al. 2002a, GeoRL, 29, 2233
Tsurutani, B. T., Galvan, C., Arballo, J. K., et al. 2002b, GeoRL, 29, 1528
Tsurutani, B. T., Guarnieri, F. L., Echer, E., Lakhina, G. S., & Verkhoglyadova, O. P. 2009, JGR, 114, A08105
Tsurutani, B. T., & Lakhina, G. S. 2004, in CP 703, Plasmas in the Laboratory and in the Universe (Melville, NY: AIP)
Tsurutani, B. T., Lakhina, G. S., Pickett, J. S., et al. 2005, NPGeo, 12, 321
Tsurutani, B. T., Lakhina, G. S., Verkhoglyadova, O. P., et al. 2011, JGR, 116, A02103
Tsurutani, B. T., Lakhina, G. S., Verkhoglyadova, O. P., Echer, E., & Guarnieri, F. L. 2010, NPGeo, 17, 467
Tsurutani, B. T., Lakhina, G. S., Winterhalter, D., et al. 1999, NPGeo, 6, 235
Turner, J. M., Burlaga, L. F., Ness, N. F., & Lemaire, J. F. 1977, JGR, 82, 1921
Winterhalter, D., Neugebauer, M., Goldstein, B. E., et al. 1994, JGR, 99, 23371
Zank, G. P., Li, G., Florinski, V., et al. 2006, JGR, 111, A06108
Zank, G. P., Rice, W. K. M., & Wu, C. C. 2000, JGR, 105, 25079